Journal of Catalysis 369 (2019) 372–381

Contents lists available at ScienceDirect

Journal of Catalysis

journal homepage: www.elsevier.com/locate/jcat

Quantitative study of the NH_3-SCR pathway and the active site distribution over $CeWO_x$ at low temperatures

Kuo Liu [a,b], Hong He [a,c,d,*], Yunbo Yu [a,c,d], Zidi Yan [a,d], Weiwei Yang [a], Wenpo Shan [a,1]

[a] State Key Joint Laboratory of Environment Simulation and Pollution Control, Research Center for Eco-Environmental Sciences, Chinese Academy of Sciences, Beijing 100085, China
[b] Editorial Office of Journal of Environmental Sciences, Research Center for Eco-Environmental Sciences, Chinese Academy of Sciences, Beijing 100085, China
[c] Center for Excellence in Regional Atmospheric Environment, Institute of Urban Environment, Chinese Academy of Sciences, Xiamen 361021, China
[d] University of Chinese Academy of Sciences, Beijing 100049, China

ARTICLE INFO

Article history:
Received 15 April 2018
Revised 4 August 2018
Accepted 25 November 2018

Keywords:
Quantitative characterization
Mechanism
$CeWO_x$
Active sites
NH_3-SCR
H_2O

ABSTRACT

The reaction and adsorption amounts of NO, NO_2, and NH_3 and the reaction pathway of the selective catalytic reduction of NO_x with NH_3 (NH_3-SCR) at low temperatures in the absence and presence of H_2O on $CeWO_x$ were quantitatively determined by a transient response method (TRM). The distribution of the active sites was quantitatively determined based on the results of TRM, X-ray photoelectron spectroscopy and temperature programmed desorption. NO_x adsorbed on O vacancies and oxidized Ce sites, with surface concentrations of 40–63 and 20 μmol g^{-1} respectively, while NH_3 adsorbed on [Ce^{4+}]-OH and W species, at 61–70 and 90–99 μmol g^{-1} respectively. Both the reaction between NO and NH_4NO_3 to form N_2, H_2O and NO_2, and reaction between nitrite and NH_3 to form N_2 and H_2O were present. H_2O weakened NH_3 adsorption, decreased the adsorption amount at 150 °C, and inhibited the reaction between NO and NH_4NO_3/adsorbed NH_3, impeding NH_3-SCR on $CeWO_x$.

1. Introduction

Nitrogen oxides (NO_x) emitted from stationary and mobile sources cause a series of environmental problems, e.g., photochemical smog, acid rain, and haze. In particular, the removal of NO_x from diesel engine exhaust attracts much attention. Academic and industrial research progress confirms that the selective catalytic reduction of NO_x with NH_3 (NH_3-SCR) is an effective method for abatement of NO_x [1]. To this aim, therefore, many efforts have been devoted to developing efficient catalysts, e.g., V-based catalysts [2], Fe- and Cu-based zeolites [3–7], Fe- and Ce-containing oxides [8–11], or discovering new ways to accelerate the reaction [12,13]. Studying the SCR mechanism is also important for the design and preparation of new catalysts. However, for these catalysts, the mechanism of NH_3-SCR has often been proposed based on qualitative studies using *in situ* diffuse reflectance infrared Fourier transform spectroscopy (DRIFTS) [14–16], transient response method (TRM) [17,18] or density functional theory (DFT) calculations [19]. Grossale et al. [20] applied the traditional TRM in quantifying the reactants and products and investigating the mechanism of the fast SCR reaction on Fe-ZSM-5 at the reaction temperatures. However, their study did not involve the adsorption steps or the distribution of the surface active components on the catalyst. So far, very few reports have quantitatively studied the distribution of the active sites of the NH_3-SCR catalysts, although quantitative determination of pathways and active sites can be of great importance, since solid evidence can be provided.

Ce-W mixed oxide catalysts have been proved to be effective for the NH_3-SCR reactions. Li's group [21] prepared a CeO_2-WO_3 catalyst, which was effective in a wide temperature range from 200 to 450 °C under a gas hourly space velocity (GHSV) 47,000 h^{-1}. The active sites for NH_3 adsorption on CeO_2-WO_3 were identified using *in situ* IR, Raman spectroscopy, temperature programmed reduction (TPR) and X-ray photoelectron spectroscopy (XPS) [22]. Shan et al. [23] developed a Ce-W oxide ($CeWO_x$) catalyst, which can remove NO completely over a wide temperature range (250–425 °C) even under the high gas hourly space velocity of 500,000 h^{-1}. Moreover, this catalyst can reduce the NO_x emission from heavy duty diesel engines sufficiently to meet the Euro V limit [24]. Using *in situ* DRIFT study, two reaction pathways, i.e., "the NH_4NO_3 path" (NO reacted with NH_4NO_3 formed by the reaction between the surface nitrates and NH_3, emitting N_2, NO_2 and H_2O) and "the nitrate path" (NO reacted with the surface nitrates to form nitrites, which would react with NH_3 to form N_2 and

* Corresponding author at: P.O. Box 2871, 18 Shuangqing Road, Haidian District, Beijing 100085, China.
E-mail address: honghe@rcees.ac.cn (H. He).
[1] Present address: Institute of Urban Environment, Chinese Academy of Sciences, Xiamen 361021, China.

https://doi.org/10.1016/j.jcat.2018.11.030
0021-9517/

H_2O), were found to be present during the standard and fast SCR reactions on $CeWO_x$ under low temperatures [15]. Until now, the reaction mechanism of NH_3-SCR on $CeWO_x$ was studied only by the qualitative study method. Also, the active site distribution on the Ce-W mixed oxides, especially on our $CeWO_x$ catalyst that was excellent under a high GHSV, is still unclear, while understanding the active site distribution can guide the design of new effective NH_3-SCR catalysts.

Water vapor is present in the combustion exhaust during practical application. It is believed that a competitive adsorption between H_2O and the reactants (NH_3/NO_x) is present on the surface of the NH_3-SCR catalysts, e.g., $Fe_{0.75}Mn_{0.25}TiO_x$, $CeMo_xZr_yO_z$ [25,26]. H_2O was found to play a negative role on NH_3-SCR over $CeWO_x$, shifting the NO_x conversion curve ~15 °C to high temperature [23], and it was inferred that this phenomenon could be attributed to the blocking of the active sites by H_2O. On the contrary, Huang et al. [27] suggested that H_2O could not reduce the adsorption of NO and NH_3 over V_2O_5/AC, but instead, the NH_3 adsorption was promoted. On this V_2O_5/AC, H_2O prohibited the reaction between the Lewis NH_3 species and NO. It seems that the effect of H_2O on the reactant (NH_3/NO_x) adsorption and the NH_3-SCR reaction mechanism depends on the nature of active metal oxides. To date, quantitative studies on the effect of H_2O vapor on the NO_x and NH_3 adsorption and the NH_3-SCR reaction mechanism at low temperatures over Ce-W mixed oxides are still lacking.

Herein, we applied TRM for quantitatively determining the NH_3-SCR reaction mechanism at low temperatures and the distribution of different active sites on $CeWO_x$, simultaneously. By using TRM, the reaction pathway of NH_3-SCR on $CeWO_x$ at low temperatures 30 and 150 °C was quantitatively determined according to the quantification of the reactants and the products, and simultaneously, the distribution of the active sites on the highly effective and promising $CeWO_x$ catalyst was clarified by combining the results of TRM, XPS and TPR. Also, the effect of H_2O on the amount of the reactant adsorption and the NH_3-SCR reaction mechanism at low temperatures was studied.

2. Experimental

2.1. Catalyst synthesis

$CeWO_x$ mixed oxide catalyst was prepared by a homogeneous precipitation method [23]. In brief, a mixed aqueous solution containing cerium nitrate ($Ce(NO_3)_3$), ammonium tungstate ($(NH_4)_{10}W_{12}O_{41}$), oxalic acid ($H_2C_2O_4$), and urea was vigorously stirred, and then heated at 90 °C for 12 h. After filtration, washing, and drying at 100 °C, the as-prepared sample was calcined at 500 °C for 5 h. The Ce/W molar ratio in $CeWO_x$ was 1:1.

2.2. Determination of the reaction/adsorption amount

The adsorption/reaction amounts of reactants were quantitatively determined by TRM (as described in Section S1.1 in Supporting Information) at low temperatures, i.e., the reaction temperature 150 °C and the room temperature 30 °C. Before the adsorption experiments, $CeWO_x$ was pretreated at 400 °C for 0.5 h by 20 vol% O_2/N_2, and then cooled down to 30 or 150 °C. Then the reactor was by-passed and the gas composition for the adsorption experiment was measured. The effluent gas was analyzed by an online NEXUS 670-FTIR spectrometer, and all spectra were recorded in a single scan with a time interval of ~8 s between scans. When the gas composition became stable, the gas was introduced into the reactor, and a curve of effluent gas composition vs. time was recorded. The adsorption figure was a function of the concentration vs. adsorption time. The amount of the adsorbed reactant can be calculated according to the ratio of the peak area to the whole area:

$$N_{ads} = \frac{A_{ads}}{A_{all}} \times N_{all}$$

where N_{ads} and N_{all} denote the number of adsorbed molecules and the overall number of molecules that were introduced into the reactor, and A_{ads} and A_{all} are the peak areas produced by N_{ads} and N_{all}, respectively.

The peaks ranging from 1911.13 to 1913.72, 1643.36 to 1644.63, 2178.72 to 2177.63, and 1120.12 to 1123.86 cm^{-1} were used for determination of the concentration of NO, NO_2, N_2O and NH_3, respectively. No overlap of NO_x and NH_3 was observed at these peak positions, as shown in Fig. S2. The peaks of N_2O_3, N_2O_4, and N_2O_5 were reported to show up at ~1830 cm^{-1} [28,29], 1750 cm^{-1} [29,30] and 1728 cm^{-1} [29], respectively. Although an NO/NO_2 mixture would mask some of the N_2O_3 features [30], the peak at 1829 cm^{-1} was not significantly overlapped by NO_2, and could be observed when the spectra of N_2O, NO_2, and N_2O_4 were digitally subtracted [28]. No peaks at 1830, 1750 or 1738 cm^{-1} were found during adsorption or reaction in this study. The correlation between the concentration of NO_x or NH_3 and the absorbance was determined using the Lamber-Beer Law:

$$A = abc$$

where A is the absorbance, a is the extinction coefficient, b is the adsorption layer thickness, and c is the concentration.

First, different fixed amounts of NO_x or NH_3 were introduced into the gas flow cell of the FTIR (Fourier transform infrared spectroscopy) instrument, and then different FTIR spectra and A values can be obtained at the steady state. The value of ab was determined by plotting A vs. c, and the slope was ab. Once the value of ab is obtained, the value of c can be calculated when A is acquired. During the adsorption process, the value of A can be obtained using FTIR. Then, the amounts of NO_x and NH_3 (c) at different time during the adsorption or reaction can be calculated according to Lamber-Beer Law. The absorbance in the spectra was measured at a resolution of 0.5 cm^{-1}, and the spectra were not treated with smoothing or noise-removing algorithm, indicating that the deviation from Beer's law might not be present [31].

The adsorption gas compositions were 500 ppm NH_3 or 500 ppm NO or 500 ppm NO_2 and N_2 balance at a total flow rate 500 mL min^{-1}. 100 mg $CeWO_x$ (40–60 mesh) was loaded into the reactor. The temperature of the catalyst was detected by a thermocouple, and the room temperature was ~30 °C. Each adsorption experiment was duplicated at least once. Especially when the adsorption amount was less than 30 μmol g^{-1}, e.g., for NO adsorption, the experiment was conducted for more than 3 times. Then, an average value with an uncertainty limit was calculated according to the values obtained.

After being treated by NH_3 or NO_2, the $CeWO_x$ catalyst was treated in N_2 flow, and some weakly adsorbed NH_3 or NO_2 was removed by N_2 flow. In order to quantify the amount of weakly adsorbed NH_3 or NO_2 that can be removed, NH_3 or NO_2 was introduced onto the surface of $CeWO_x$ again, and the adsorption amount during the second adsorption process was equal to the amount that could be removed by N_2.

Blank experiments were also carried out. In these experiments, no catalyst was loaded in the reactor, and the experimental procedure was the same as that introduced above. It was found that the consumption amounts of NO, NO_2, and NH_3 were ~0 mol g^{-1} at both 30 and 150 °C, as shown in Fig. S3.

Temperature programmed surface reaction (TPSR) was performed on the pretreated $CeWO_x$ in 500 ppm NO/N_2 or 500 ppm NO/N_2 + 2 vol% H_2O, with a heating rate of 10 °C min^{-1}. The gas flow rate was 500 mL min^{-1}, and the amount of catalyst was

100 mg (40–60 mesh). The effluent gas was analyzed by an online NEXUS 670-FTIR spectrometer, and the spectra were recorded in a single scan with a time interval of ~8 s between scans.

3. Results and discussion

3.1. NO_2 adsorption

First, introducing NO_2 onto the surface of fresh $CeWO_x$ resulted in a drastic decrease in the NO_2 concentration (~100 μmol g^{-1}), accompanied by an increase in the NO concentration (~40 μmol g^{-1}) at 30 °C (Fig. 1). No N_2O, N_2O_3, N_2O_4, or N_2O_5 was observed. The molar ratio between the consumed NO_2 and the formed NO was 2.625:1. It was reported that three NO_2 molecules could form one NO molecule (NO_2:NO = 3:1) on zeolites [17] or on TiO_2 [32], while other researchers found that during NO_2 disproportionation reaction, two NO_2 molecules formed one NO molecule (NO_2:NO = 2:1) [33]. However, the ratio of NO_2 consumption to NO formation was <3:1 but >2:1 in the present study. Therefore, it is reasonable to conclude that Eqs. (1) [34], (4) and (5) took place [17]:

$$NO_2 + NO_2 + [Ce^{3+}]\text{-}\square \leftrightarrow [Ce^{4+}]\text{-}ONO_2 + NO \quad (1)$$

where $[Ce^{3+}]$-□ is an O vacancy Ce site, the presence of which was observed in our previous study using XPS [23]. Eq. (1) is the NO_2 disproportionation reaction, and might be a combination of the following equations:

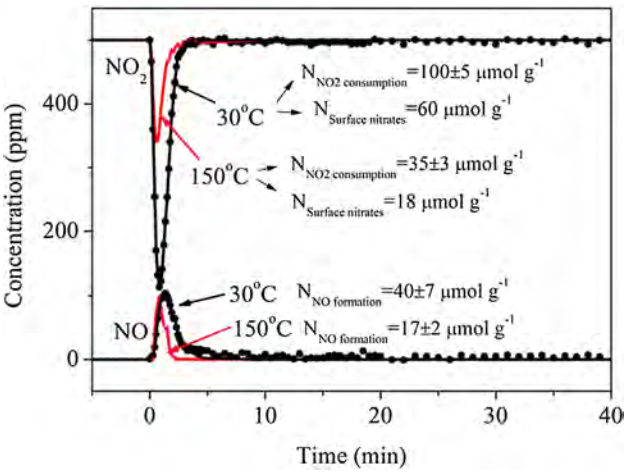

Fig. 1. 500 ppm NO_2 adsorption over $CeWO_x$ at 30 and 150 °C.

$$NO_2 + [Ce^{3+}]\text{-}\square \leftrightarrow [Ce^{4+}]\text{-}ONO \quad (2)$$

$$[Ce^{4+}]\text{-}ONO \leftrightarrow NO + [Ce^{4+}]\text{-}O \quad (3)$$

$$[Ce^{4+}]\text{-}O + NO_2 \rightarrow [Ce^{4+}]\text{-}ONO_2 \quad (4)$$

It is difficult to detect the nitrite species ($[Ce^{4+}]$-ONO) since the nitrites are highly reactive and are inclined to desorb from the surface of $CeWO_x$ [15]. Similarly, Kijlstra et al. [35] found that nitrite species formed on MnO_x/Al_2O_3 were less thermodynamically stable than the nitrate species. Thus, the equations above were derived based on speculation.

Mutual transformation takes place between monodentate, bidentate and bridging nitrates (($[Ce^{4+}]$-$O)_2$ = NO) [15] (Eq. (S1)). Eqs. (1) and (S1) show that the two NO_2 molecules can react on $CeWO_x$ to form one surface nitrate and one NO molecule.

$$[Ce^{4+}]\text{-}O + NO_2 \rightarrow [Ce^{4+}]\text{-}ONO_2 \quad (4)$$

$$[Ce^{4+}]_2\text{-}O_2 + NO_2 \rightarrow [Ce^{4+}]\text{-}ONO_2 + [Ce^{4+}]\text{-}O \quad (5)$$

where $[Ce^{4+}]$-O and $[Ce^{4+}]_2$-O_2 denote a lattice oxygen and an adsorbed oxygen, respectively.

Eqs. (4) and (5) are the NO_2 adsorption. In the case of NO_2 adsorption (Eqs. (4) and (5)), no NO molecules can be detected in the outlet gas, and all consumed NO_2 forms surface nitrates.

The amount of NO_2 consumed to form NO by NO_2 disproportionation (Eq. (1)) was:

$$N_{NO2-equation(1)} = 2N_{NO\ formation} = 2 \times 40\ \mu mol\ g^{-1} = 80\ \mu mol\ g^{-1}$$

where N denotes the number of molecules. The amounts of NO_2 consumed by NO_2 adsorption (Eqs. (4) and (5)) and the formed surface nitrate were calculated to be 20 and 60 μmol g^{-1}, respectively (Section S2.1.2 in Supporting Information), indicating that at 30 °C, the surface nitrates formed by NO_2 adsorption on $[Ce^{3+}]$-□ and oxidized Ce sites were 40 and 20 μmol g^{-1}, as shown in the Scheme 1.

At 150 °C, the amounts of NO_2 consumption and NO evolution were 35 and 17 μmol g^{-1}, respectively, lower than those at 30 °C, indicating that some weakly adsorbed species were absent. The amount of NO_2 consumption decreased at 150 °C, possibly due to the acceleration of the reverse reaction of NO_2 disproportionation (Eq. (1)). Since the peaks of monodentate nitrates (1527 and 1271 cm^{-1}) were lower at 150 °C in comparison with those at 30 °C according to DRIFTS results (Fig. S4), it can be concluded that the weakly adsorbed species were partly monodentate nitrates [16]. The molar ratio of NO_2/NO was 2:1 at 150 °C. Since the ratio of NO_2 consumption to NO emission during NO_2 disproportionation (Eq. (1)) is 2:1, whereas that during NO_2 adsorption (Eqs. (4) and (5)) is 1:0, it can be concluded that only NO_2 disproportiona-

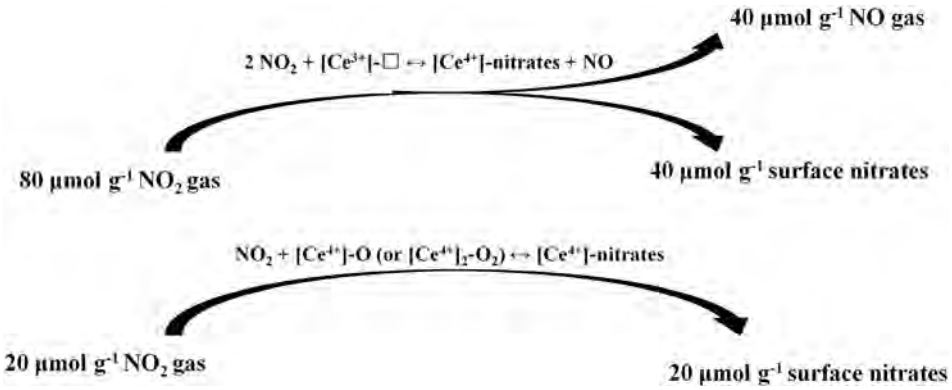

Scheme 1. Surface nitrates formed by NO_2 adsorption on $[Ce^{3+}]$-□ and oxidized Ce sites at 30 °C.

tion (Eq. (1)) occurred at 150 °C, and NO_2 adsorbed following Eqs. (1) and (S1) at 150 °C. The absence of NO_2 adsorption (Eqs. (4) and (5)) at 150 °C suggests that the nitrates formed on oxidized Ce sites ($[Ce^{4+}]$-O and $[Ce^{4+}]_2$-O_2) by NO_2 adsorption were weakly adsorbed nitrates (20 μmol g^{-1}), since the weakly adsorbed nitrates would desorb from the $CeWO_x$ surface to form NO_2 at a higher temperature. Thus, $[Ce^{3+}]$-□ was the site for nitrate formation during the SCR reaction, whereas $[Ce^{4+}]$-O and $[Ce^{4+}]_2$-O_2 did not participate in the formation of nitrates.

3.2. Reaction between NO gas and the adsorbed NO_2

After N_2 purge, NO gas was introduced onto the surface of $CeWO_x$ saturated with the nitrates formed by NO_2 adsorption at 30 and 150 °C. The amount of weakly adsorbed NO_2 removed by N_2 flow was negligible (Fig. S5). At 30 °C, upon feeding NO into the reactor, the amount of NO decreased, with the evolution of NO_2 (Fig. 2a). To exclude the possibility of NO_2 production by NO oxidation, NO adsorption on fresh $CeWO_x$ was also conducted, and no NO_2 was evolved (Fig. 2b). It is obvious that the amount of surface nitrates formed by NO_2 (60 μmol g^{-1}) was ~6 times of that formed by NO in terms of amount. Analogously, Sivachandiran et al. [32] reported that no significant adsorption of NO was observed on TiO_2, whereas about 2.2–12 μmol m^{-2} NO_2 was consumed during the adsorption process. Seen from Fig. 2a, the amount of NO adsorbed (10 μmol g^{-1}) was smaller than that on NO_2-presorbed $CeWO_x$ (25 μmol g^{-1}), indicating that reaction between NO and the nitrate species to form NO_2 gas was present.

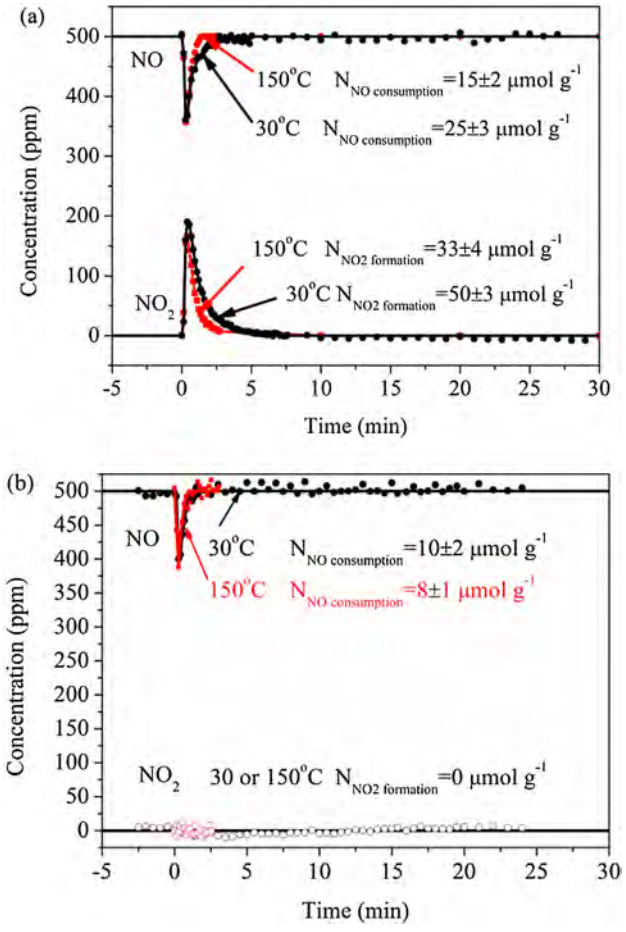

Fig. 2. 500 ppm NO adsorption over $CeWO_x$ pre-treated in 500 ppm NO_2 in N_2 (a) and over fresh $CeWO_x$ (b) at 30 and 150 °C.

According to the DRIFT results in our previous study [15], monodentate, bidentate, and bridging nitrates were found to be present during NO adsorption on $CeWO_x$ at 150 °C. Tang et al. [36] reported the presence of the transformation between different nitrates on MnO_x/TiO_2. Therefore, it can be suggested that nitrate formation (Eqs. (6) and (7)) and the transformation among the monodentate, bidentate and bridging nitrates (Eq. (S1)) were present during NO adsorption:

$$NO + 2[Ce^{4+}]\text{-}O \leftrightarrow [Ce^{4+}]\text{-}ONO + [Ce^{4+}]\text{-}O \leftrightarrow ([Ce^{4+}]\text{-}O)_2 = NO \quad (6)$$

$$NO + [Ce^{4+}]_2\text{-}O_2 \leftrightarrow ([Ce^{4+}]\text{-}O)_2 = NO \quad (7)$$

Quantitative analysis showed that the ratio between the NO_2 production (50 μmol g^{-1}) and NO consumption (25 μmol g^{-1}) was 2:1, and hence, Eq. (8) can be suggested:

$$NO + [Ce^{4+}]\text{-}ONO_2 \leftrightarrow NO_2 + [Ce^{4+}]\text{-}ONO \leftrightarrow 2NO_2 + [Ce^{3+}]\text{-}□ \quad (8)$$

Although surface nitrite ($[Ce^{4+}]$-ONO) might be formed, this species was so unstable that it dissociated into NO_2 gas once it was formed.

At 30 °C, after the reaction between NO and the nitrates (Eq. (8)) took place, about 25 μmol g^{-1} nitrates, part of which were monodentate nitrates (Fig. S4), desorbed to form NO_2, and the remaining surface nitrate concentration was 35 μmol g^{-1} (Sections S2.1.3, S2.2 and Fig. S6 in Supporting Information), indicating that about half of the nitrate was reactive and unstable at 30 °C. At 150 °C (Fig. 2a), the amounts of NO consumption and NO_2 emission were 15 and 33 μmol g^{-1}, respectively. The amount of the nitrate species formed during NO_2 adsorption was 18 μmol g^{-1} at 150 °C (Fig. 1), indicating that almost all the stable nitrates in Fig. S6 could react with NO gas to form NO_2.

3.3. Reaction between the NO and the adsorbed NH_3 after NO_2 adsorption

The reaction between NH_3 and NO_2 was also quantitatively determined. The amount of NH_3 adsorbed on NO_2-preadsorbed $CeWO_x$ was 220 μmol g^{-1} at 30 °C (Fig. 3a), which was 60 μmol g^{-1} more than that on fresh $CeWO_x$ (160 μmol g^{-1}). Since the NO_2 adsorption formed 60 μmol g^{-1} of surface nitrates (Fig. 1), it can be inferred that NH_3 could react with the surface nitrates to form NH_4NO_3, leading to a 60 μmol g^{-1} increase in the adsorption amount of NH_3. Our previous DRIFT study found that NO_2 could react with NH_3 to form NH_4NO_3 at room temperature on $CeWO_x$ [15]. Hence, one NH_3 molecule can react with one nitrate:

$$NH_3 + [M^{n+}]\text{-}OH \leftrightarrow [M^{n+}]\text{-}O\text{-}NH_4 \quad (9)$$

$$[M^{n+}]\text{-}O\text{-}NH_4 + [Ce^{4+}]\text{-}ONO_2 \leftrightarrow [M^{n+}]\text{-}O\text{-}NH_4NO_3\text{-}[Ce^{4+}] \quad (10)$$

where $[M^{n+}]$-OH denotes a Brønsted acid site, and M^{n+} denotes a Ce^{4+} or W^{n+}.

It can be suggested that NH_3 and NO_2 adsorbed on different sites, so that the presence of the surface nitrates could increase the amount of NH_3 adsorption by forming NH_4NO_3. It was reported by Li's group [22] that on CeO_2-WO_3, NH_3 could be adsorbed weakly on CeO_2 at the Lewis acid sites and strongly on WO_x at the Lewis acid sites and the hydroxyl formed on $Ce_2(WO_4)_3$ at the Brønsted acid sites. Joshi et al. [37] investigated the NH_3 adsorption on CeO_2 and CeO_2/W by density functional theory (DFT) calculations, and found that the NH_3 adsorption at the Lewis acid sites of CeO_2 (1 1 1) surface, either clean or doping with W, was weak (<21 kJ/mol), but NH_3 bound strongly at the Brønsted acid sites. Therefore, it is reasonable to conclude that NH_3 could

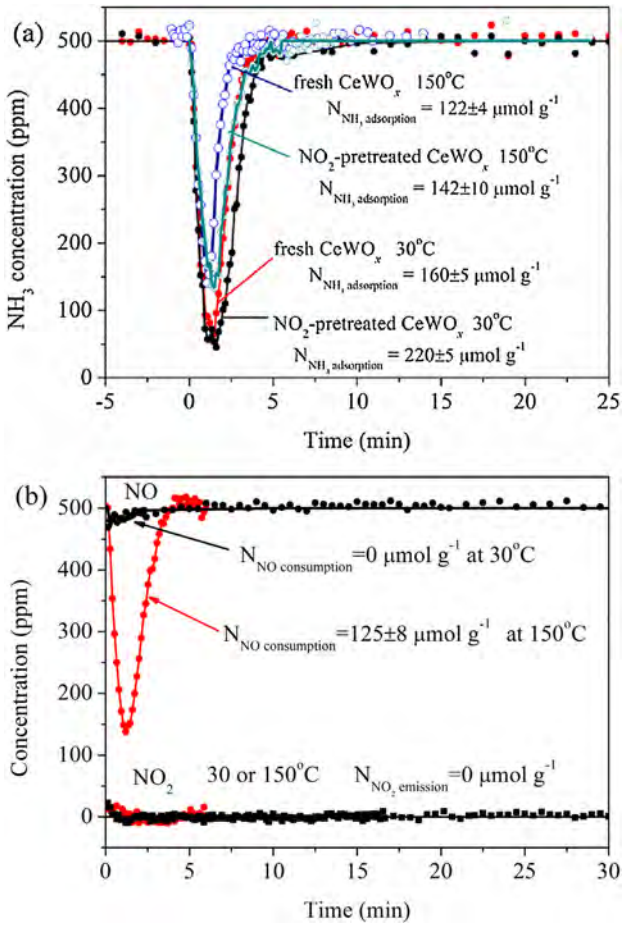

Fig. 3. (a) 500 ppm NH_3 adsorption at 30 and 150 °C on fresh $CeWO_x$ and on $CeWO_x$ pretreated in 500 ppm NO_2 in N_2 until saturation and then purged by N_2; (b) 500 ppm NO adsorption at 30 and 150 °C on $CeWO_x$ saturated first by NO_2 and then by NH_3.

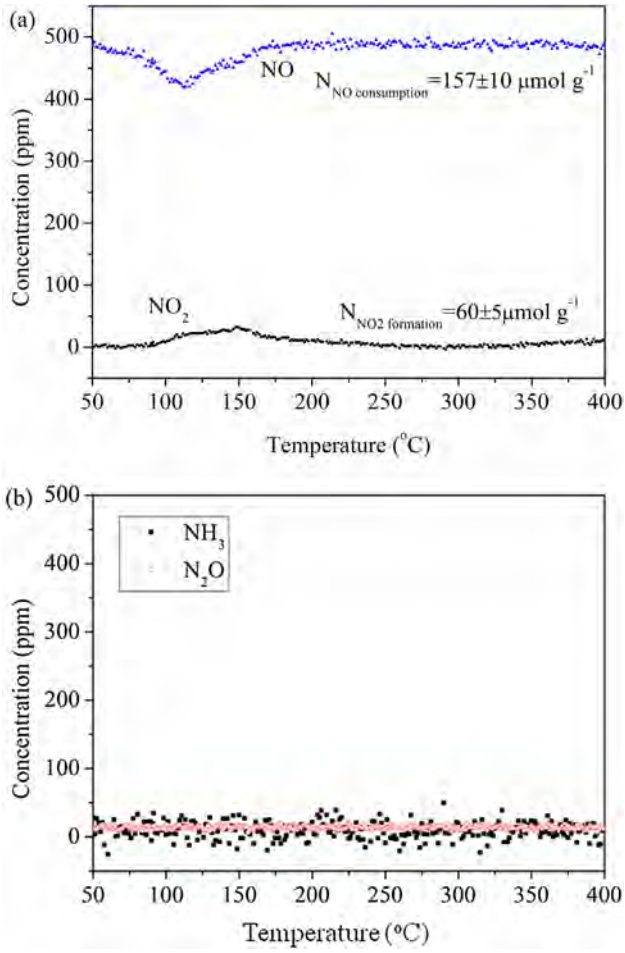

Fig. 4. TPSR of $CeWO_x$ in 500 ppm NO pretreated by 500 ppm NO_2 and then 500 ppm NH_3 at room temperature.

be adsorbed on the Lewis acid sites consisting of W species, and also on the Brønsted sites consisting of Ce species neighboring W atoms ([Ce^{4+}]-OH) and W-OH sites in $Ce_2(WO_4)_3$, the overall amount of which was 160 μmol g^{-1}. The information above of identifying the nature of the active sites obtained from the literature can be applied in the quantification of the active site distribution on $CeWO_x$.

When NO was subsequently introduced into the reactor at 30 °C, almost no NO was consumed on this NH_4NO_3-covered catalyst (Fig. 3b), indicating that NO gas could not react with the surface nitrates to form NO_2 due to the formation of NH_4NO_3 [18]. Similarly, Grossale et al. [17] found that the presence of NH_3 prohibited the reaction between NO and the surface nitrates by forming ammonia nitrates on Fe-zeolite, raising the reaction temperature.

The successive TPSR results showed that the consumption of NO started below 100 °C, and a maximum conversion of NO was observed at ~115 °C (Fig. 4), indicating that NO can react with NH_4NO_3 below 150 °C [15]. According to the above discussion, 60 μmol g^{-1} NH_4NO_3 was formed in this process, and the remaining amount of adsorbed NH_3 after N_2 purge was 101 μmol g^{-1} (Fig. S5). The quantification of NO consumption and NO_2 evolution during TPSR was 157 and 60 μmol g^{-1}, respectively, indicating that 60 μmol g^{-1} NH_4NO_3 and 100 μmol g^{-1} NH_3 could react with 157 μmol g^{-1} NO at the ratios of NO/NH_4NO_3/NO_2 1/1/1 and NO/NH_3 1/1, as shown in Eqs. (11) and (12).

$$4NO + 4(\text{adsorbed } NH_3) + 2(O \text{ atom}) \rightarrow 4\ N_2 + 6H_2O \quad (11)$$

$$[M^{n+}]\text{-O-}NH_4NO_3\text{-}[Ce^{4+}] + NO \rightarrow N_2 + NO_2 + H_2O + [M^{n+}]\text{-OH} + [Ce^{4+}]\text{-OH} \quad (12)$$

where [M^{n+}]-OH denotes a Brønsted acid site, and M^{n+} denotes a Ce^{4+} or W^{n+}.

Eq. (11) does not involve evolution of NO_2, and could be the overall reaction for the following series of reactions:

$$NO + [Ce^{4+}]\text{-O} \leftrightarrow [Ce^{4+}]\text{-ONO} \quad (13)$$

$$[Ce^{4+}]\text{-ONO} + [M^{n+}]\text{-}NH_3 \rightarrow N_2 + H_2O + [Ce^{4+}]\text{-OH} + [M^{n+}] \quad (14)$$

$$[Ce^{4+}]\text{-ONO} + [M^{n+}]\text{-O-}NH_4 \rightarrow N_2 + H_2O + [Ce^{4+}]\text{-OH} + [M^{n+}]\text{-OH} \quad (15)$$

where [M^{n+}] denotes a Lewis acid site and M^{n+} denotes a metal site.

It should be noted that it is difficult to detect the nitrite species ([Ce^{4+}]-ONO) since they are unstable and highly active toward the adsorbed NH_3 on $CeWO_x$, as pointed out in our previous study [15]. Analogously, Wang et al. [14] pointed out that it was difficult to detect the nitrite species using DRIFTS on Cu-SAPO-34, partly due to its high reactivity toward NH_3. Many researchers suggested the presence of the reaction concerning the nitrites since it also contributed to the SCR reaction [14,18,38]. Wang et al. [14] included the reaction between the nitrites and NH_3 in the

NH_3-SCR mechanism on Cu-SAPO-34. Kijlstra et al. [38] proved the presence of the reaction between the NH_2 species and the reactive nitrite intermediates at low temperatures below 473 K on MnO_x/Al_2O_3. Nova et al. [18] pointed out that NO_2 disproportionated on V_2O_5-WO_3/TiO_2 to produce nitrates and nitrites, and the nitrites could react with NH_3 to form ammonium nitrite and further N_2. Therefore, reactions involving the nitrite species ([Ce^{4+}]-ONO) were also included in the NH_3-SCR mechanism in this study.

At 150 °C, the amount of NH_3 adsorbed on NO_2-preadsorbed $CeWO_x$ was 20 μmol g^{-1} more than that on fresh $CeWO_x$ (Fig. 3a). To identify if NH_3 could react with the nitrates adsorbed on $CeWO_x$ at 150 °C, *in situ* DRIFT spectra were taken at 150 °C upon passing 500 ppm NH_3 over the NO_2-presorbed $CeWO_x$. As seen in Fig. S7, after the introduction of NH_3, the peaks of the surface nitrates decreased, indicating that the nitrates could react with NH_3 at 150 °C. After 5 min, the peaks of the nitrates disappeared and only NH_3 peaks were observed. Therefore, it can be concluded that all nitrates (18 μmol g^{-1}) could react with NH_3 at 150 °C. When NO was introduced onto the surface of $CeWO_x$ subsequently, the amounts of NO consumption and NH_3 adsorption were 125 and 117 μmol g^{-1} (Figs. 3b and S5), respectively, indicating that all the adsorbed NH_3 could participate in the SCR reaction at 150 °C. The ratio of NO consumption to NH_3 adsorption was about 1:1, indicating that the reaction between NO and the adsorbed NH_3 (Eq. (11)) took place at 150 °C.

At this point, a clear picture of the active site distribution and the reaction pathway of both standard and fast SCR at 150 °C on $CeWO_x$ can be drawn, as shown in Fig. 5. The surface of $CeWO_x$ was covered mostly by NH_3, and the amount of surface nitrates formed by NO_2 (60 μmol g^{-1}) was ~6 times greater than that formed by NO at 30 °C (Table 1). It should be noted that the composition of the catalyst has to be calculated based on the data collected at 30 °C, since the composition of the catalyst won't change with the increase in the temperature. With an increase in the temperature, the only change is the amount of the adsorbed species. Some weakly adsorbed species will desorb from the surface at higher temperatures, and the vacant active sites are just spectators and won't take part in the reaction. Thus, at 150 °C, some active sites did not participate in the reaction (Table 1) due to the weak interactions between the reactants and catalyst, e.g., the surface [Ce^{4+}]-O did not adsorb NO_2, only a part of the [Ce^{3+}]-□ sites activated NO_2 to form [Ce^{4+}]-ONO_2 and NO gas. To calculate the active site distribution, the different active sites should be clarified first. NH_3 could be adsorbed on the Lewis acid sites consisting of W

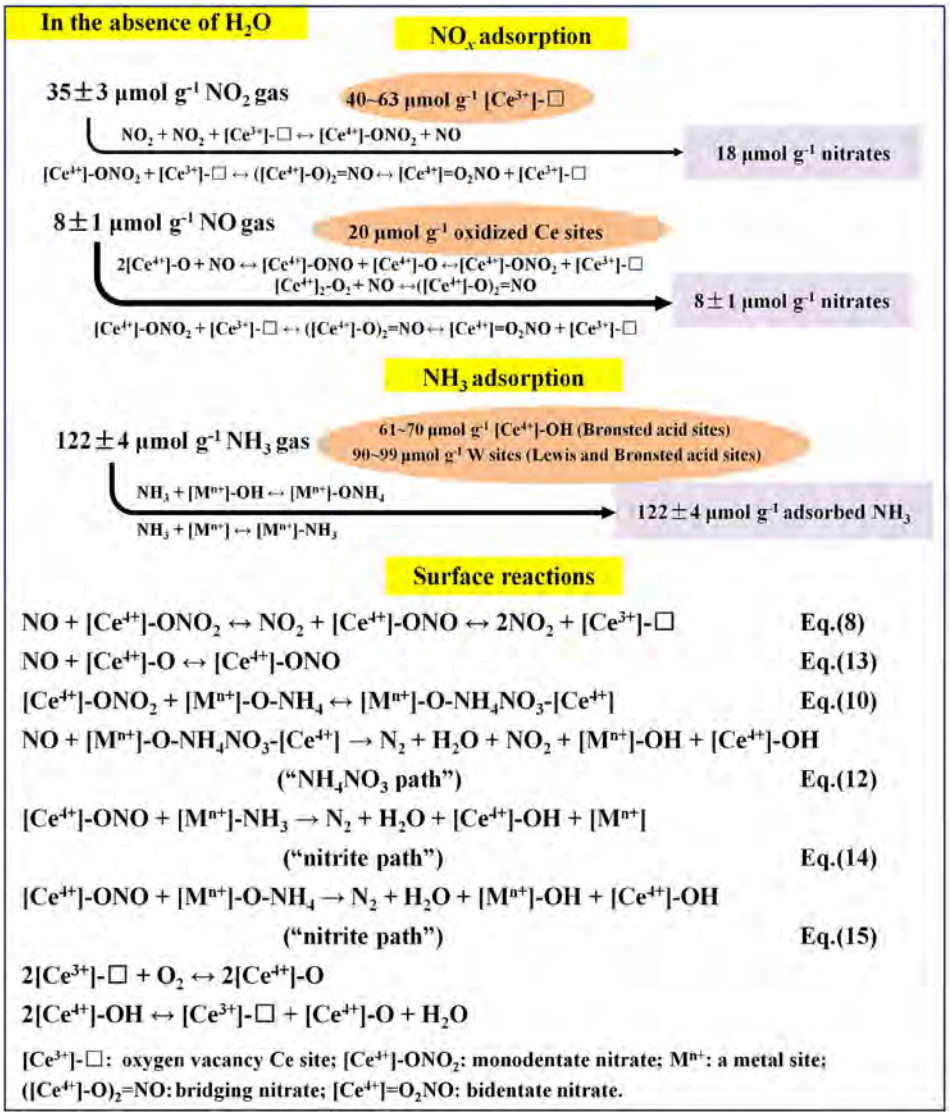

Fig. 5. Mechanism of NH_3-SCR over $CeWO_x$ in the absence of H_2O at 150 °C.

Table 1
Summary of the NO, NO_2 and NH_3 adsorption amounts on $CeWO_x$.

Conditions	Temperature	NO	NO_2	NH_3
In the absence of H_2O	30 °C	10 μmol g^{-1}	$[Ce^{4+}]$-O + $[Ce^{4+}]_2$-O_2: 20 μmol g^{-1} $[Ce^{3+}]$-□: 40 μmol g^{-1}	160 μmol g^{-1}
	150 °C	8 μmol g^{-1}	$[Ce^{3+}]$-□: 18 μmol g^{-1}	122 μmol g^{-1}
In the presence of H_2O	30 °C	20 μmol g^{-1}	H_2O: 86 μmol g^{-1}	245 μmol g^{-1}
	150 °C	33 μmol g^{-1}	$[Ce^{3+}]$-□: 16 μmol g^{-1}	90 μmol g^{-1}

species, and also on the Brønsted sites consisting of Ce species neighboring W atoms ($[Ce^{4+}]$-OH) and W-OH sites in $Ce_2(WO_4)_3$, whereas NO_2 could be adsorbed on $[Ce^{3+}]$-□ and oxidized Ce sites including $[Ce^{4+}]$-O and $[Ce^{4+}]_2$-O_2. According to the Ce/W atomic ratio (Table S1) and the $Ce^{3+}/(Ce^{3+}+Ce^{4+})$ concentration [23] obtained by XPS, the amounts of $[Ce^{3+}]$-□, oxidized Ce sites, $[Ce^{4+}]$-OH and W species were calculated to be 40–63, 20, 61–70, and 90–99 μmol g^{-1} (For detailed calculation procedure please refer to Section S2.1.4 in Supporting Information), i.e., 0.342–0.538 $[Ce^{3+}]$-□ nm^{-2}, 0.171 oxidized Ce nm^{-2}, 0.521–0.598 $[Ce^{4+}]$-OH nm^{-2}, and 0.769–0.845 W nm^{-2}, respectively. To confirm that the value of the active site amount was correctly calculated, the amount of W in this study was compared with that calculated in the literature. Iwasaki et al. [39] pointed out that the NO reduction rate on WO_3/CeO_2 catalysts correlated closely with the W density when the theoretical W density was in the range of 0–10 W nm^{-2}. The W density calculated in the present study (0.769–0.845 W nm^{-2}) was within the range of that (0–10 W nm^{-2}) reported by Iwasaki et al. [39], indicating that the surface active site distribution calculated in this study had a correct order of magnitude, and is believable. The amounts of (monodentate + bidentate) and bidentate nitrates formed on $CeWO_x$ could also be calculated, at 17 and 23 μmol g^{-1} (For detailed calculation procedure please refer to Section S2.1.4), respectively.

According to Eqs. (6)-(15) and (S1), both the "NH_4NO_3 path", i.e. the reaction between NO and NH_4NO_3, and the "nitrite path", i.e. the reaction between nitrite and the adsorbed NH_3, were present during the standard and fast SCR. These results confirm our previous conclusions drawn by the *in situ* DRIFTS results [15], indicating that the method in this study can be applied in studying the NH_3-SCR mechanism at low temperatures. However, it should be noted that the NO adsorption resulted in much less nitrates than NO_2 adsorption (Table 1), indicating that the "NH_4NO_3 path" might not play an important role due to the lack of NO_2 and the resulting lack of NH_4NO_3 during standard SCR. The "nitrite path" during standard SCR has been reported by many other researchers. Liu et al. [40] studied the standard SCR mechanism on W-doped CeO_2 catalysts using DFT calculations, and found the presence of the "nitrite path" during the standard SCR. The "nitrite path" was also reported to be present during standard SCR on a Mn/Fe-Ti spinel catalyst at low temperatures by Yang et al. [41]. Cheng et al. [42] suggested that the Langmuir-Hinshelwood (L-H) mechanism, i.e., the reaction between NO_2 and NH_4^+ ("nitrite path"), was involved in the standard SCR reaction on Cu-Mn/ZSM and Cu-Mn/SAPO-34. Bendrich et al. [43] found that the standard SCR mechanism involved the "nitrite path" on Cu-CHA. Therefore, it is reasonable to conclude that the "nitrite path" contributed to standard SCR on $CeWO_x$.

3.4. Reaction mechanism of NH_3-SCR in the presence of H_2O

Since H_2O is present under realistic reaction conditions, the effect of H_2O on the adsorption of NO_2, NH_3, and the NH_3-SCR reaction was also investigated using TRM. No N_2O, N_2O_3, N_2O_4, or N_2O_5 was observed during this adsorption/reaction process. Seen from Fig. 6, the pre-adsorption of H_2O increased the amounts of the NO_2 and NH_3 adsorption at 30 °C. As seen in Fig. 6a, the molar ratio between the consumed NO_2 and the formed NO was ~3:1 (129:44), indicating that Eq. (16) was present.

$$3NO_2 + H_2O \leftrightarrow 2HNO_3 + NO \quad (16)$$

The molar ratio between the NO_2 consumption and NO emission in the presence of H_2O (~3:1) was different from that in the absence of H_2O (~2:1) at 30 °C, suggesting that the NO_2 adsorption pathway was changed by H_2O. It is possible that the adsorption of H_2O covers the surface of $CeWO_x$, and NO_2 mainly adsorbed on H_2O molecules, leading to the presence of Eq. (16). Grossale et al. [17] reported that the molar ratio of NO formed and NO_2 consumed was 1:3 in the presence of H_2O over Fe-zeolite catalysts, and Eq. (16) contributes to the adsorption of NO_2 on Fe-zeolite catalysts in the presence of water. The reaction between NO_2 and H_2O taking place at 30 °C during NO_2 adsorption on $CeWO_x$ was similar to that on Fe-zeolite in the presence of H_2O since the NO_2/NO ratio values on $CeWO_x$ and Fe-zeolite were both 3:1.

However, at 150 °C, the NO_2 adsorption amount decreased slightly, and the molar ratio between the consumed NO_2 and the formed NO was 2:1 (32:16), indicating that Eq. (1) took place, and H_2O occupied a small amount of the active site for NO_2 adsorption at the reaction temperature. Similarly, Nova et al. [44] proposed that two NO_2 molecules could react with one H_2O molecule at the reaction temperature in the presence of H_2O on a commercial V_2O_5-WO_3/TiO_2 catalyst. Thus, the NO_2 adsorption in the presence of H_2O at 150 °C followed the same pathway (Eq. (1)) as that in the absence of H_2O.

The presence of H_2O increased the NO adsorption amounts at both 30 and 150 °C (Fig. 6c). However, as seen in Fig. S8b, most of the NO molecules could easily be removed by N_2 purge at either 30 or 150 °C, and it could be concluded that NO molecules were weakly adsorbed on the H_2O pretreated $CeWO_x$. Liu et al. [26] found that the amount of surface adsorbed NO species decreased when H_2O was introduced onto the surface of $Fe_{0.75}Mn_{0.25}TiO_x$, and ascribed this phenomenon to a competitive adsorption between H_2O and NO. A similar conclusion that H_2O could inhibit the adsorption of NO and impede active nitrate species formation on the surface of Mn-Fe/TiO_2 was drawn by Zhu et al. [45]. However, in the present study, a competitive adsorption between NO and H_2O was not observed, but instead, H_2O weakened the adsorption of NO. The weakly adsorbed NO species were easily to be removed by N_2 (Fig. S8b). Most of the surface NO species were weakly adsorbed in the presence of H_2O (much more weakly adsorbed than that in the absence of H_2O, Fig. S8b), leading to a decreased NH_3-SCR activity.

As seen in Fig. 6b and Table 1, the amount of NH_3 adsorbed at 30 °C increased by about 85 μmol g^{-1}, whereas the NH_3 adsorption amount at 150 °C decreased by 32 μmol g^{-1} in comparison with that in the absence of H_2O. This indicates that the presence of H_2O could facilitate the weakly adsorbed NH_3 at 30 °C. It was reported that hydrogen bond originating from the interaction between a hydrogen atom and an electron rich atom, like N, was always present in chemical and biological processes, e.g., in the

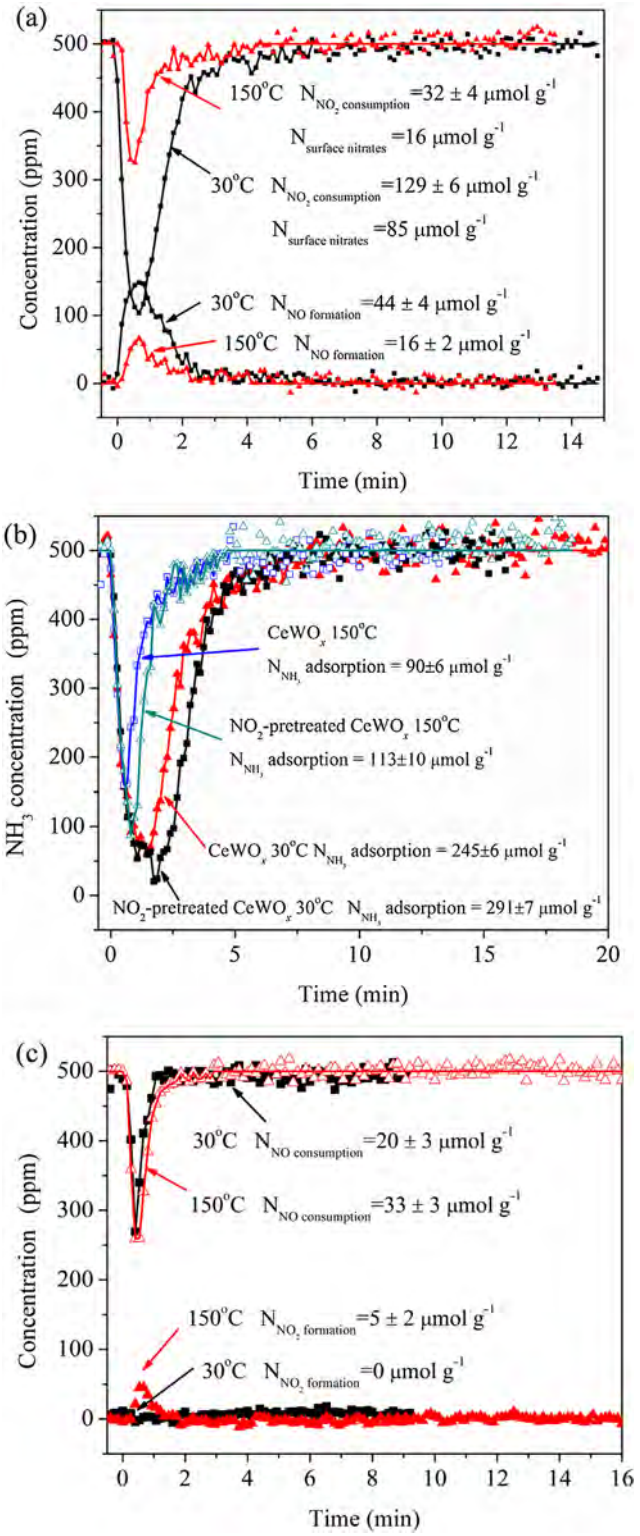

Fig. 6. (a) 500 ppm NO_2 and (b) 500 ppm NH_3 adsorption on 2 vol% H_2O pretreated $CeWO_x$, and (c) 500 ppm NO + 2 vol% H_2O adsorption over fresh $CeWO_x$ at 30 and 150 °C.

system containing NH_3 and H_2O [46–49]. Latajka and Scheiner [47] pointed out that the H_3N-HOH binding energy was <6 kcal mol^{-1} based on DFT calculations, and Del Bene [48] found that the value was <8 kcal mol^{-1}, indicating that the H_3N-HOH interaction was weak. Therefore, the promotion of the weakly adsorbed NH_3 in this study was ascribed to the formation of the H_3N-HOH interaction [49]. Nevertheless, when the temperature was increased to 150 °C, the weakly adsorbed NH_3 molecules desorbed from the surface, resulting in a decrease in the NH_3 adsorption amount. Many studies [25,26,50] reported that the presence of H_2O occupied the active sites for NH_3 adsorption, and a competitive adsorption between H_2O and NH_3 was present. This conclusion originated from the decreased NH_3 amount observed in the presence of H_2O [25,26,50]. However, the present study found that the decrease of NH_3 adsorption was not due to the competitive adsorption of NH_3 and H_2O, but was because of the interaction between NH_3 and H_2O (H_3N-HOH) weakening the NH_3 adsorption, which resulted in a larger amount of NH_3 desorption at 150 °C, and further, a decrease in the NH_3 adsorption amount at the reaction temperature (150 °C). Our previous study pointed out that W promoted the NH_3-SCR reaction on $CeWO_x$ through promoting the NH_3 adsorption capacity [23]. Also, it was reported that the surface acidity of the Ce-based catalysts, i.e., the site for NH_3 adsorption, was an important factor for NH_3-SCR [51], and the NH_3-SCR activity increased with the increasing surface acid content. Therefore, less NH_3 participating in NH_3-SCR at 150 °C was one of the reasons for the decrease in the NH_3-SCR activity in the presence of H_2O on $CeWO_x$.

It can be proposed that NH_3 adsorption on the $CeWO_x$ follows the equations:

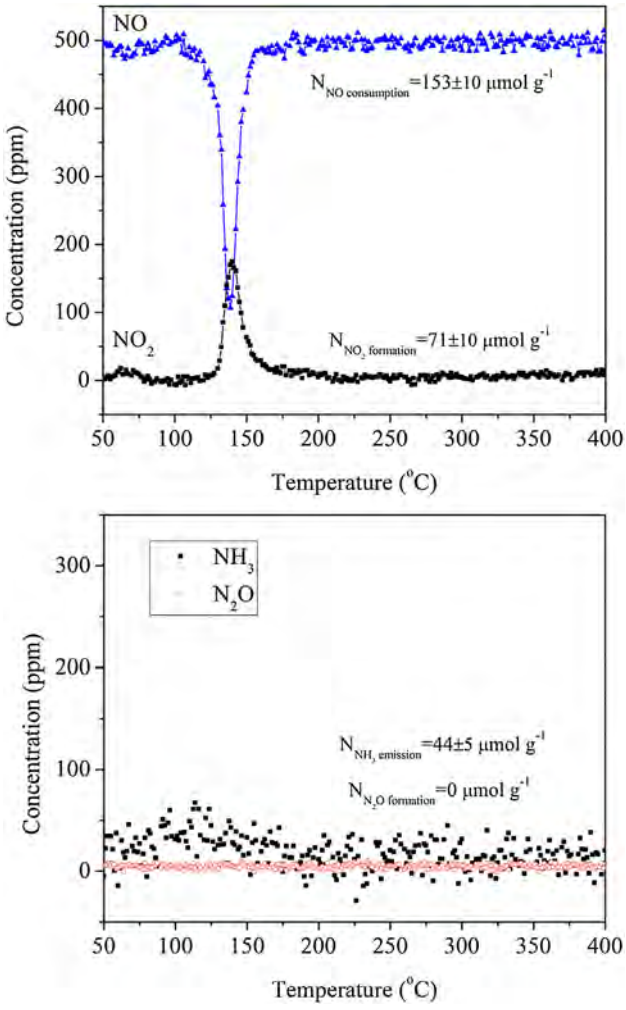

Fig. 7. TPSR in 500 ppm NO + 2% H_2O of $CeWO_x$ pretreated by 2 vol% H_2O, 500 ppm NO_2 and then 500 ppm NH_3 at 30 °C.

$$NH_3 + [M^{n+}]\text{-}OH \leftrightarrow [M^{n+}]\text{-}ONH_4 \quad (9)$$

$$NH_3 + [M^{n+}] \leftrightarrow [M^{n+}]\text{-}NH_3 \quad (17)$$

where $[M^{n+}]$-OH and $[M^{n+}]$ denote a Brønsted acid site and a Lewis acid site, respectively, and M^{n+} denotes a metal site.

The results of TPSR in NO and H_2O of $CeWO_x$ pretreated in the H_2O, NO_2 and NH_3 successively are shown in Fig. 7. Since the NO_2 adsorption formed 85 μmol g^{-1} of surface nitrates (Fig. 6a), it is possible that 85 μmol g^{-1} NH_4NO_3 was formed at 30 °C, while the remaining amount of adsorbed NH_3 at 30 °C was 214–85 = 129 μmol g^{-1} (Fig. S8). The amounts of NO consumption, NO_2 and NH_3 evolution during TPSR were 159, 71, and 44 μmol g^{-1} (Fig. 7), respectively, indicating that 85 μmol g^{-1} NH_4NO_3 and 85 μmol g^{-1} NH_3 could react with 159 μmol g^{-1} NO at the ratios of NO/NH_4NO_3/(NO_2 emission) 1/1/1 (71/71/71) (Eq. (12)), NO/NH_3 1/1 (68/68) (Eq. (11)), and NO/NH_4NO_3/NH_3 1/1/1 (14/14/14) (Eqs. (10), (18) and (14)-(15)). Therefore, it can be proposed that the following equations are present during NH_3-SCR in the presence of H_2O:

Formation and decompostion of NH_4NO_3:

$$[M^{n+}]\text{-}ONH_4 + [Ce^{4+}]\text{-}ONO_2 \leftrightarrow [M^{n+}]\text{-}ONH_4NO_3\text{-}[Ce^{4+}] \quad (10)$$

NO reacted with NH_4NO_3 to form N_2 and NO_2:

$$NO + [M^{n+}]\text{-}ONH_4NO_3\text{-}[Ce^{4+}] \leftrightarrow NO_2 + N_2 + H_2O + [M^{n+}]\text{-}OH + [Ce^{4+}]\text{-}OH \quad (12)$$

Reaction between NO and nitrates:

$$NO + [Ce^{4+}]\text{-}ONO_2 + [Ce^{3+}]\text{-}\square \leftrightarrow 2[Ce^{4+}]\text{-}ONO \quad (18)$$

Reactions between the adsorbed NH_3 and the nitrite species:

$$[Ce^{4+}]\text{-}ONO + [M^{n+}]\text{-}NH_3 \rightarrow N_2 + H_2O + [Ce^{4+}]\text{-}OH + [M^{n+}] \quad (14)$$

$$[Ce^{4+}]\text{-}ONO + [M^{n+}]\text{-}ONH_4 \rightarrow N_2 + H_2O + [Ce^{4+}]\text{-}OH + [M^{n+}]\text{-}OH \quad (15)$$

where M^{n+} denotes a metal site.

It should be noted that the NO_2 adsorption, the reaction between NO and the surface nitrates, the reaction between the nitrates and the adsorbed NH_3, and the reaction between NO and NH_4NO_3 (formed by the reaction between NH_3 and the nitrates produced from NO_2 adsorption) were studied in this study. These reactions are typical reactions when NO_2 is present in the reaction gas feed, i.e., under fast SCR conditions. Therefore, the mechanism studied was for describing both standard and fast SCR.

In summary, the standard and fast NH_3-SCR reaction pathways in the presence of H_2O are shown in Fig. 8. The reaction pathways of NH_3-SCR in the presence of H_2O are similar to those in the absence of H_2O (Fig. 5), including both the "nitrite path" and "NH_4NO_3 path". Similar to the discussion above in Section 3.3, since the NO adsorption led to much less strong-adsorbed nitrates than NO_2 adsorption in the presence of H_2O, it is possible that the "NH_4NO_3 path" might not play an important role during standard SCR in the

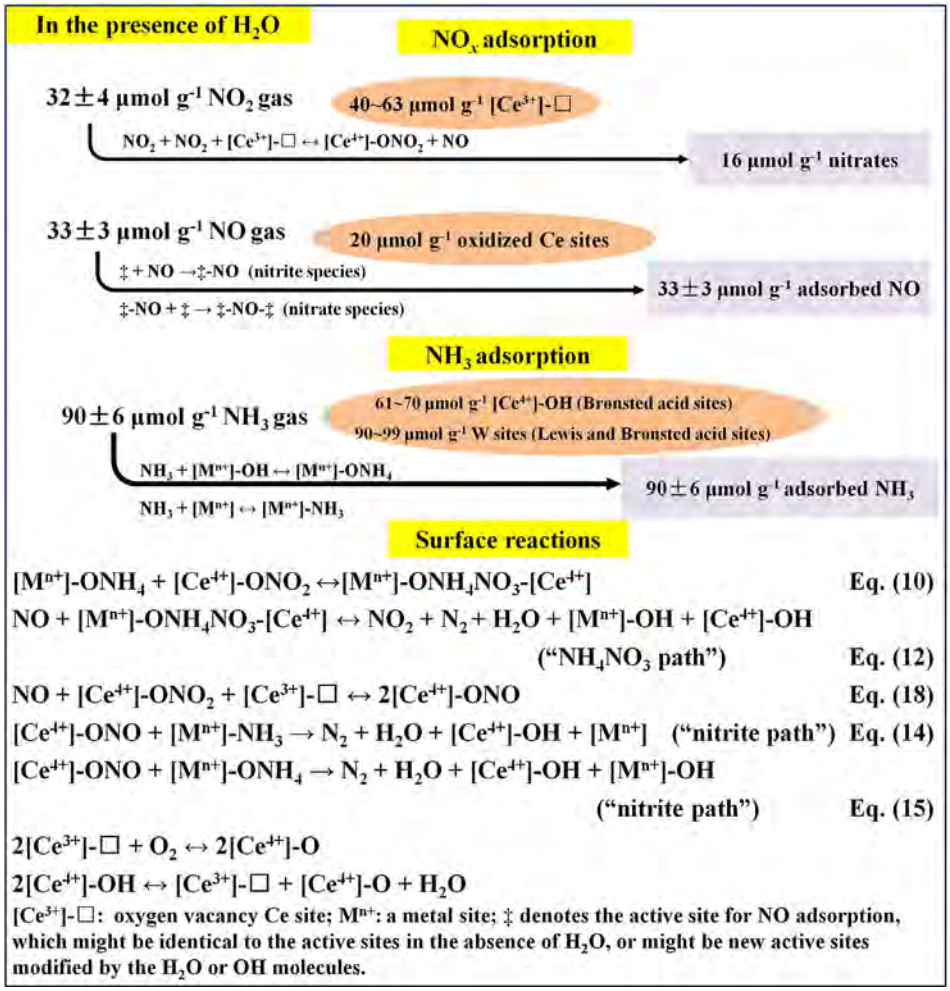

Fig. 8. Mechanism of NH_3-SCR over $CeWO_x$ in the presence of H_2O at 150 °C.

presence of H_2O, which is similar to the mechanism in the absence of H_2O. Seen in Fig. 7, in the presence of H_2O, NH_3 desorbed below 100 °C, demonstrating that NH_3 preferred desorbing to reacting with NO, consistent with the conclusion drawn from Fig. 6 that the NH_3 adsorption was weakened by H_2O. The amounts of the adsorbed active surface NO and NH_3 species decreased greatly due to the presence of H_2O, impeding the "nitrite path" reactions. Also, during TPSR in NO and H_2O, a maximum consumption of NO was observed at ~140 °C (Fig. 7), higher than that in the absence of H_2O (~115 °C, Fig. 4), indicating that the presence of H_2O inhibited the reaction between NO and NH_4NO_3/the adsorbed NH_3. Similarly, Xiong et al. [50] found that H_2O could reduce the oxidation ability of a low temperature SCR Mn-Fe spinel catalyst, inhibiting NO oxidation to NO_2 and the reaction between the adsorbed NH_3 and NO, which led to a lower NH_3-SCR reaction rate in the presence of H_2O. Huang et al. [27] reported that H_2O prohibited the reaction between the adsorbed NH_3 on Lewis acid sites and NO on V_2O_5/AC, decreasing the SCR activity. Overall, both the weaker adsorption of NH_3/NO at the reaction temperature and the inhibition of the reaction between NO and NH_4NO_3/the adsorbed NH_3 resulted in a decreased NH_3-SCR activity in the presence of H_2O on $CeWO_x$.

4. Conclusions

In summary, the adsorption amount of NH_3 on $CeWO_x$ was much greater than that of NO_x. NO_x adsorbed on $[Ce^{3+}]$-□ and oxidized Ce sites ($[Ce^{4+}]$-O and $[Ce^{4+}]_2$-O_2), at 40–63 and 20 μmol g^{-1} respectively, while NH_3 adsorbed on $[Ce^{4+}]$-OH and W species, at 61–70 and 90–99 μmol g^{-1}, respectively. At the reaction temperature, both the "NH_4NO_3 path", i.e. the reaction between NO and NH_4NO_3 to form N_2, H_2O and NO_2, and the "nitrite path", i.e. the reaction between nitrite and the adsorbed NH_3 to form N_2 and H_2O, were present on $CeWO_x$, both in the absence and presence of H_2O. The presence of H_2O weakened the adsorption of NO/NH_3 on $CeWO_x$, leading to a decrease in the adsorption amounts of the active species at 150 °C, and further, a decrease in the NH_3-SCR activity. Moreover, H_2O inhibited the reaction between NO and the adsorbed NH_3 species on $CeWO_x$, leading to a lower NH_3-SCR activity.

Conflicts of interest

None.

Acknowledgements

This work was financially supported by the National Key R&D Program of China (2017YFC0211101), the National Natural Science Foundation of China (21303247 and 21637005) and the China Postdoctoral Science Foundation (2012M520018).

Appendix A. Supplementary material

Detailed information on the experimental setup (Fig. S1), XPS (Table S1), FTIR (Fig. S2), *in situ* DRIFTS (Figs. S4 and S7), TPD (Fig. S6) results, blank adsorption experiment (Fig. S3), the determination of the different surface species amounts (Figs. S5 and S8) and the active site distribution (Section S2) is included. Supplementary data to this article can be found online at https://doi.org/10.1016/j.jcat.2018.11.030.

References

[1] T.V. Johnson, Int. J. Engine Res. 10 (2009) 275–285.
[2] R.Q. Long, R.T. Yang, Appl. Catal. B 24 (2000) 13–21.
[3] J. Ma, Z.C. Si, X.D. Wu, D. Weng, Y. Ma, J. Environ. Sci. 41 (2016) 244–251.
[4] F. Gao, N.M. Washton, Y. Wang, M. Kollar, J. Szanyi, C.H.F. Peden, J. Catal. 331 (2015) 25–38.
[5] L.J. Xie, F.D. Liu, K. Liu, X.Y. Shi, H. He, Catal. Sci. Technol. 4 (2014) 1104–1110.
[6] A. Sultana, T. Nanba, M. Haneda, M. Sasaki, H. Hamada, Appl. Catal. B 110 (2010) 61–67.
[7] K. Wijayanti, K. Leistner, S. Chand, A. Kumar, K. Kamasamudram, N.W. Currier, A. Yezerets, L. Olsson, Catal. Sci. Technol. 6 (2016) 2565–2579.
[8] P.L. Wang, H.Q. Wang, X.B. Chen, Y. Liu, X.L. Weng, Z.B. Wu, J. Mater. Chem. A 3 (2015) 680–690.
[9] X.L. Mou, B.S. Zhang, Y. Li, L.D. Yao, X.J. Wei, D.S. Su, W.J. Shen, Angew. Chem. Int. Ed. 51 (2012) 2989–2993.
[10] X. Li, J.H. Li, Y. Peng, H.Z. Chang, T. Zhang, S. Zhao, W.Z. Si, J.M. Hao, Appl. Catal. B 184 (2016) 246–257.
[11] X.Q. Wang, A.J. Shi, Y.F. Duan, J. Wang, M.Q. Shen, Catal. Sci. Technol. 2 (2012) 1386–1395.
[12] Z.W. Huang, X. Gu, W. Wen, P.P. Hu, M. Makkee, H. Lin, F. Kapteijn, X.F. Tang, Angew. Chem. Int. Ed. 52 (2013) 660–664.
[13] P. Forzatti, I. Nova, E. Tronconi, Angew. Chem. Int. Ed. 48 (2009) 8366–8368.
[14] D. Wang, L. Zhang, K. Kamasamudram, W.S. Epling, ACS Catal. 3 (2013) 871–881.
[15] K. Liu, F.D. Liu, L.J. Xie, W.P. Shan, H. He, Catal. Sci. Technol. 5 (2015) 2290–2299.
[16] L. Chen, J.H. Li, M.F. Ge, Environ. Sci. Technol. 44 (2010) 9590–9596.
[17] A. Grossale, I. Nova, E. Tronconi, J. Catal. 265 (2009) 141–147.
[18] I. Nova, C. Ciardelli, E. Tronconi, D. Chatterjee, B. Bandl-Konrad, AIChE J. 52 (2006) 3222–3233.
[19] C. Paolucci, A.A. Verma, S.A. Bates, V.F. Kispersky, J.T. Miller, R.G. Gounder, W. N. Delgass, F.H. Ribeiro, W.F. Schneider, Angew. Chem. Int. Ed. 53 (2014) 11828–11833.
[20] A. Grossale, I. Nova, E. Tronconi, D. Chatterjee, M. Weibel, J. Catal. 256 (2008) 312–322.
[21] L. Chen, J.H. Li, M.F. Ge, L. Ma, H.Z. Chang, Chin. J. Catal. 32 (2011) 836–841.
[22] Y. Peng, K.Z. Li, J.H. Li, Appl. Catal. B 140–141 (2013) 483–492.
[23] W.P. Shan, F.D. Liu, H. He, X.Y. Shi, C.B. Zhang, Chem. Commun. 47 (2011) 8046–8048.
[24] W.P. Shan, F.D. Liu, Y.B. Yu, H. He, C.L. Deng, X.Y. Zi, Catal. Commun. 59 (2015) 226–228.
[25] S.P. Ding, F.D. Liu, X.Y. Shi, K. Liu, Z.H. Lian, L.J. Xie, H. He, ACS Appl. Mater. Interfaces 7 (2014) 9497–9506.
[26] F.D. Liu, H. He, Catal. Today 153 (2010) 70–76.
[27] Z.G. Huang, Z.Y. Liu, X.L. Zhang, Q.Y. Liu, Appl. Catal. B 63 (2006) 260–265.
[28] R.H. Kagann, A.G. Maki, J. Quant. Spectrosc. Radiat. Transf. 31 (2) (1984) 173–176.
[29] K.I. Hadjiivanov, Catal. Rev. – Sci. Eng. 42 (1–2) (2000) 71–144.
[30] C.H. Bibart, G.E. Ewing, J. Chem. Phys. 61 (1974) 1293–1299.
[31] L. Shao, P.R. Griffiths, P.M. Chu, T.W. Vetter, Appl. Spectrosc. 60 (3) (2006) 254–260.
[32] L. Sivachandiran, F. Thevenet, P. Gravejat, A. Rousseau, Appl. Catal. B 142–143 (2013) 196–204.
[33] J.A. Rodriguez, T. Jirsak, G. Liu, J. Hrbek, J. Dvorak, A. Maiti, J. Am. Chem. Soc. 123 (2001) 9597–9605.
[34] Y. Lu, H. Chen, J. Phy. Chem. C 118 (2014) 10043–10052.
[35] W.S. Kijlstra, D.S. Brands, E.K. Poels, A. Bliek, J. Catal. 171 (1997) 208–218.
[36] N. Tang, Y. Liu, H.Q. Wang, Z.B. Wu, J. Phys. Chem. C 115 (2011) 8214–8220.
[37] A. Joshi, A. Rammohan, Y. Jiang, S. Ogunwumi, J. Mol. Struct.: Theochem. 912 (2009) 73–81.
[38] W.S. Kijlstra, D.S. Brands, H.I. Smit, E.K. Poels, A. Bliek, J. Catal. 171 (1997) 219–230.
[39] M. Iwasaki, K. Dohmae, Y. Nagai, E. Sudo, T. Tanaka, J. Catal. 359 (2018) 55–67.
[40] B. Liu, J. Liu, S. Ma, Z. Zhao, Y. Chen, X.-Q. Gong, W. Song, A. Duan, G. Jiang, J. Phys. Chem. C 120 (2016) 2271–2283.
[41] S. Yang, F. Qi, S. Xiong, H. Dang, Y. Liao, P.K. Wong, J.H. Li, Appl. Catal. B 181 (2016) 570–580.
[42] M. Cheng, B. Jiang, S. Yao, J. Han, S. Zhao, X. Tang, J. Zhang, T. Wang, J. Phys. Chem. C 122 (2018) 455–464.
[43] M. Bendrich, A. Scheuer, R.E. Hayes, M. Votsmeier, Appl. Catal. B 222 (2018) 76–87.
[44] I. Nova, C. Ciardelli, E. Tronconi, D. Chatterjee, Catal. Today 114 (2006) 3–12.
[45] L. Zhu, Z.P. Zhong, H. Yang, C.H. Wang, Water Air Soil Pollut. 227 (2016) 476.
[46] P.A. Kollman, L.C. Allen, Chem. Rev. 72 (3) (1972) 283–303.
[47] Z. Latajka, S. Scheiner, J. Phys. Chem. 94 (1990) 217–221.
[48] J.E. Del Bene, J. Phys. Chem. 92 (1988) 2874–2880.
[49] P.A. Stockman, R.E. Bumgarner, S. Suzuke, G.A. Blake, J. Chem. Phys. 96 (4) (1992) 2496–2510.
[50] S.C. Xiong, Y. Liao, X. Xiao, H. Dang, S.J. Yang, Catal. Sci. Technol. 5 (2015) 2132–2140.
[51] L. Zhang, J. Sun, L. Li, S. Ran, G. Li, C. Li, C. Ge, L. Dong, Ind. Eng. Chem. Res. 57 (2018) 490–497.